Wind tunnel tests for vortex generators mitigating leading-edge roughness on a 30% thick airfoil

Gutiérrez, R.; Llórente, E.; Echeverría, F.; Ragni, D.

Important note
To cite this publication, please use the final published version (if applicable).
Please check the document version above.

PAPER • OPEN ACCESS

Wind tunnel tests for vortex generators mitigating leading-edge roughness on a 30% thick airfoil

Wind tunnel tests for vortex generators mitigating leading-edge roughness on a 30% thick airfoil

R Gutiérrez[1], E Llorente[1], F Echeverria[1] and D Ragni[2]

[1]Nordex Energy Spain S.A.U, Avenida Ciudad de la Innovación 3, 31621 Sarriguren, Navarra, Spain.

[2]Aerodynamics, Wind Energy, Flight Performance and Propulsion Department, Faculty of Aerospace Engineering, Delft University of Technology, Kluyverweg 1, 2629, HS Delft, the Netherlands.

E-mail: `RGutierrez@nordex-online.com`

Abstract. In this study, the aerodynamic performance of a thick airfoil is analysed, after installing leading-edge roughness to emulate a severe state on the airfoil surface. The impact on aerodynamic coefficients has been quantified using two roughness methods: zig-zag tape and sandpaper. Wind tunnel tests are carried out at a Reynolds number of $3 \cdot 10^6$. At low angles of attack, zig-zag tape and sandpaper provide comparable lift and drag coefficients but significant variations of these coefficients are obtained for high angles of attack. Stalled flow is the cause of the most significant variation on the airfoil performance between smooth and rough surface states. Vortex generators are adapted to recover the lift coefficient value previously given by the airfoil under smooth conditions. As a result, vortex generators are able to reduce the loss of lift and the sensitivity of the airfoil to the rough state.

1. Introduction

The exposure of a Horizontal Axis Wind Turbine (HAWT) to atmospheric and environmental conditions substantially alters the designed performance of the machine. Different sources of surface deterioration and erosion have been reported by insects, hail, sand grains, etc. Their combination determines a modification of the blade surface from its design geometry. As a result, a reduction of annual energy production (AEP) is obtained along with a direct increase in the cost of energy (COE).

As it is highlighted by Erhmann [1], the amount of power loss depends on the wind turbine controller scheme. Stall regulated wind turbines have their blades designed to reach stall at high wind speeds. The resulting lift loss produces a power regulation only dependant on the blade aerodynamics which can be significantly affected by the presence of roughness. This type of wind turbines experiences power losses of the order of 25% as it was measured by Corten [2] due to insects depositions on a 700kW wind turbine blade. Pitch regulated wind turbines can suffer from power losses of the order of 5% instead for the same causes. Erhmann [1] demonstrated that pitch regulation reduces the roughness impact on power production, as the main power losses were found in the quadratic power curve region.

Nowadays there is not a standardized method for testing roughness which impedes a reliable and accurate comparison even when the same roughness heights are employed. The review done by F. Zidane et al. [3] collects several results from both experimental and numerical studies.

From their work, it is concluded that a limited number of publications have introduced system identification to predict the wind turbine blade performance under different surface roughness conditions.

ZigZag tapes (ZZ tapes) have been traditionally used for promoting turbulent transition of boundary layers (BL). The transition anticipation produced by roughness can be emulated with the use of ZZ tapes. This setup mostly depends on the tape height and the relative location of the tape on both suction and pressure airfoil sides. For example, Fuglsang et al. [4] used ZZ tapes at 5% on the suction side (SS) and 10% on the pressure side (PS) while Timmer et al. [5] used only ZZ tape at 5% on the suction side. In fact, the relative location of the tapes is determined by previous experience and it is not directly related to a realistic measure of the surface state. Ehrmann [1] and White [6] stated that ZZ tapes are not representative of distributed roughness.

The NACA standard method [7] is a widespread technique to emulate distributed roughness on an airfoil leading-edge. Carborundum grains are spread between the first 8% of the airfoil chord length (c) at both airfoil sides covering a density between 5 and 10%. Nevertheless, the method has low repeatability due to the manual deposition of the carborundum, which is dependent on the procedure. B.Mendez et al. [8] tried to characterize a given carborundum distribution to use the empirical correlation of Van Rij et al. [9] on Computational Fluid Dynamics (CFD) simulations. The difficulty in characterizing a rough surface was stated due to the variation of the obtained distribution and the density covered. In fact, even the single carborundum elements change in shape for the same grit number.

Sandpaper has been recently employed on airfoils to emulate a rough surface. The bonding of sandpaper to an airfoil leading-edge accurately replicates the roughness distribution used on tests, but it introduces a severe rough state. O.Pires et al. [7] tested different sandpapers attached on an airfoil of 18% of thickness to assess the carborundum grain size and the sandpaper extension influence. Afterwards, an scaled sandpaper setup was used in the blade tip region of a wind turbine. As a result, an AEP loss of 5% was related to the sandpaper presence.

The main physical effects produced by roughness elements when used to emulate a severe surface state on the airfoil leading-edge is the change of the characteristics of the boundary layer upstream of the element itself among which the anticipation of turbulent boundary layer transition. Turner et al. [10] performed flow visualization for showing turbulent BL transition anticipation on turbomachine blades. Other studies [11], [12] have revealed that the boundary layer turbulence properties are also modified from the airfoil leading-edge by roughness. An increment of turbulence intensity on the surface is usually measured. Expected effects on airfoil performance are a decrement of maximum lift coefficient (C_L), a change in C_L slope and an increment of drag coefficient (C_D). These effects are not fully emulated by ZZ tapes as the flow is not modified upstream of the ZZ tape locations.

This article aims the variation of the aerodynamic impact produced by roughness methods on a thick airfoil. With this purpose, different methods have been used.

A thick airfoil has been selected for this study. As remarked by Timmer et al. [13], blade manufacturers tend to use thick airfoils in a large portion of the blade. These kinds of airfoils are typically characterized by more structural stiffness so a reduction of blade weight can be done along with a consequent reduction of fatigue loads and costs.

For the same roughness state and angle of attack (AoA), stronger adverse pressure gradients can be produced on relatively thick airfoil geometries compared to thin airfoils. This can determine the presence of stalled flow. Timmer et al. [13] emphasized the sensitivity to nose roughness of the pressure side of thick airfoils.

Vortex generators (VGs) are passive flow control devices widely known to be quite effective in delaying trailing-edge separation due to a re-energization of the boundary layer. Baldacchino et al. [14] performed a parametric experimental study about passive vortex generators on a 30%

thick airfoil under smooth and tripped conditions using a ZZ tape on 5%SS. Skrzypinski et al. [15] provided BEM computations for demonstrating an AEP recovery due to the use of vortex generators under rough conditions.

In this study, the VGs position is adapted to reduce the deviation in airfoil performance once a different roughness method is used (i.e., using VGs on the airfoil pressure side if it is needed).

2. Experimental setup

2.1. Wind tunnel

An experimental study has been carried out in the Low-Speed Low-Turbulence Wind Tunnel (LSLT) of the Delft University of Technology. This is an atmospheric tunnel of the closed-throat single-return type, with a contraction ratio of 17.8. It has a 2.9 m diameter six-bladed fan driven by a 525 kW DC motor, giving a maximum test section velocity of about 120 m/s. For all tests, a Reynolds number (Re) of $3 \cdot 10^6$ was kept by a free stream velocity of 75m/s with a turbulence level of 0.07%.

The test section is 1.80 m wide, 1.25 m high and 2.60 m long. Electrically actuated turntables flush with the test-section top and bottom walls provide positioning and support to a two-dimensional model in the middle of the test section length, as it is shown in Figure 1. The centre of rotation of the model explained in paragraph 2.2 is set at the half chord. The tested angle of attack range is defined between -20º and 20º.

Infrared thermography cameras (IR) were used to visualize transition meanwhile the tests were carried out. It was ensured not to have undesired dirt which could produce bypass transition on the airfoil.

2.2. Model and instrumentation

The airfoil model has a chord length of 0.6 m and a span length of 1.25 m. The model manufactured in glass fibre and resin, was installed in the test section as it is shown in Figure 1.

Figure 1. Left: airfoil model on wind tunnel test section. Right: stereoscopic PIV setup for trailing-edge measurements on the airfoil suction side.

The pressures were measured by a DTC INITIUM system containing ESP scanners. A total number of 90 pressure taps were used on the model to obtain the aerodynamic coefficients. The acquisition frequency of the system was 330 Hz and averaged every 127 samples during a total averaging time of 10 s.

A wake-rake of pitot tubes was installed downstream the airfoil to obtain C_D based on loss momentum method [16]. Static and total pressure probes placed in two different rows were used to carry out the measurements. Both rows had a width of 504 mm and were located $0.82c$ downstream of the trailing edge of the model. A total number of 16 probes were used for measuring static pressure and 67 for measuring total pressure. The spacing between total pressure probes varies from 3 mm over 96 mm in the rake centre to 6, 12 and 24 mm towards both ends of the rake.

Besides, stereoscopic PIV measurements were carried out at the middle of the airfoil span. Seeding particles from SAFEX-Long-Lasting-Mix were generated by a SAFEX fog machine able to provide droplets with a median diameter of 1 μm. Particles of these diameters are found not to provide with relevant uncertainties due to particle-slip with the measured accelerations [17]. The tracer droplets have been injected downstream the model with the aim of determining an uniform and homogeneous concentration at the test section after flow recirculation in the closed circuit. Laser light provided by a Quantel CFR200 Nd:Yag laser with 200 mJ pulse^{-1} has been used to form a laser sheet of about 35 cm width approximately 2 mm thick at the field of view (FOV) location (see Figure 1). The flow is imaged by two sCMOS cameras with a sensor resolution of 2560x2160 px^2, 16 bit, pixel size 6.5 μm. The two cameras are mounted with a relative angle of 37$^{\text{o}}$, respectively, at about 10$^{\text{o}}$ forward scatter. Two Nikon–Nikkor lenses of f = 180 mm focal length and aperture f/5.6 are mounted on the sCMOS cameras. Image acquisition, processing and post-processing have been carried out by the LaVision DaVis 8.1.5 software. For each angle of attack, 500 images have been acquired and further processed by a multi-pass correlation algorithm. An error lower than 1% is expected with this set-up concerning the results from [18].

2.3. Roughness methods

ZZ tape and sandpaper were chosen as the roughness methods to be used. A severe distributed roughness state is tested on the model leading-edge using sandpaper.

ZZ tapes were attached to the first 5% on model SS and the first 10% on PS, as in Fuglsang [4]. To evaluate the influence of this method on thick airfoils PS, a test with only ZZ tape on 5%SS is included. Braslow method [19] was used in order to obtain an indicative critical height of the tape for forcing turbulent boundary layer transition. Finally, a height of 0.4 mm is used for each configuration. The turbulent transition promotion carried out by the ZZ tape was checked by IR images.

The airfoil model was additionally tested with sandpaper installed from the leading-edge to the first 8%c on both airfoil sides. The same extension is used in the NACA standard method [7]. O.Pires et al. [20] used this extension and any inconveniences were reported for the sandpaper method. However, the main difference between the sandpaper and the NACA standard method is the carborundum grains distribution density. Typically sandpaper presents higher density which was not provided by the sandpaper manufacturer. A sandpaper with a grit number of 100 was selected with a nominal grain size of 162 μm according to the FEPA-Standard 42-1:2006 [21].

2.4. Vortex generators setup

Triangular VGs have been used for the most highly separated cases. VGs vanes are placed to produce downstream vortexes with a counter-rotating movement between the vortexes produced by each vane. Only the streamline vortex generator position is varied. Experimental studies as

[14], revealed that a suitable position is to locate the VGs array on the suction side at the 30% of the chord (c). Due to the present roughness sensitivity on the airfoil pressure side, VGs are also used on the airfoil pressure side at a location of 30%c for the sandpaper test and at 40%c for the ZZ tape test. VGs are installed at a more upstream location for the sandpaper test to cope with the severe lift loss produced by the method. The relation between the boundary layer thickness δ and the VGs height h_{VG} is such that $h_{VG}/\delta > 1$.
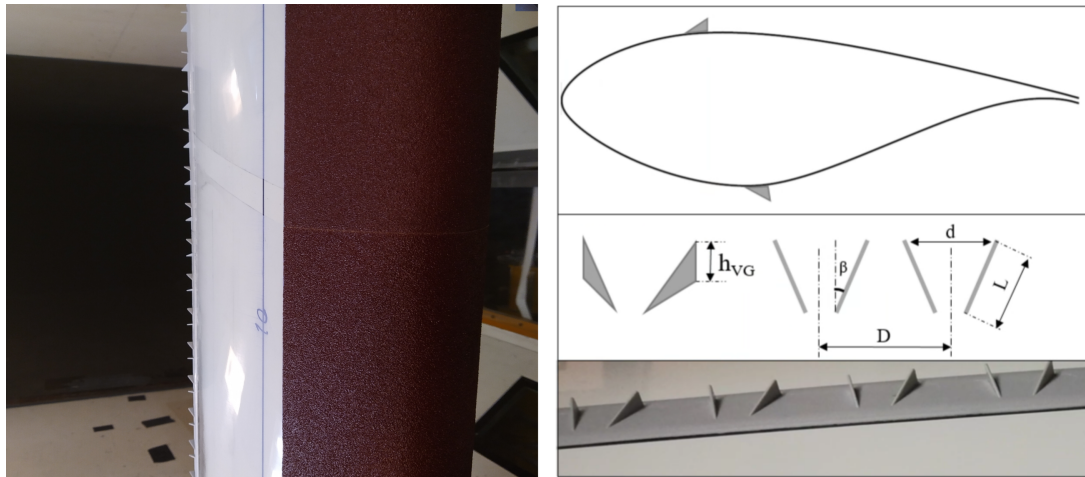

Figure 2. Left: sandpaper attached on model leading-edge and VGs on 30%SS. Right: sketch of triangular VGs. Note that the sketch is not in true magnitude as the real VGs height is around 1% of the airfoil chord length. Dimensions can not be provided due to confidentiality reasons.

Consequently, the test matrix of this study can be defined by table 1.

Table 1. Test matrix.

Roughness add-on	x/c on SS	x/c on PS	VGs x/c on SS	VGs x/c on PS
ZigZag tape	5%	-	-	-
	5%	10%	-	-
	5%	10%	-	40%
	5%	10%	30%	40%
Sandpaper 100	8%	8%	-	-
	8%	8%	-	30%
	8%	8%	30%	40%

3. Results
Due to confidentiality reasons, plot tick-marks have been reduced.

3.1. ZZ tape method sensitivity
The sensitivity of the ZZ tape method is analysed using two ZZ tape setups, 5SS and 5SS 10PS. Both setups have a ZZ tape attached on the airfoil suction side at a location of 5%c. The main

difference between both setups is the use of a ZZ tape on the airfoil pressure side at a location of 10%c. These setups are based on the ones used in other researches [4] and [5].

In Figure 3 the ZZ tapes setups are compared with the airfoil clean state. The influence of the ZZ tape on the suction side is in concordance with other studies such as [13]. A reduction of maximum C_L is obtained along with a slope change in the linear part of C_L polar curve. These effects were related to the extension of turbulent flow produced by the forced transition of the ZZ tape. The increase in boundary layer thickness is reflected by the C_D value which was mostly increased in the positive AoA range.

On the other side, once a ZZ tape is used on the airfoil pressure side a significant deviation between the setups is obtained in terms of aerodynamic coefficients. A similar maximum C_L is reached for both ZZ tape cases, but for positives AoAs a lower C_L value is obtained with the use of ZZ tapes on both model sides. Near positive stall, the C_D increment is similar for both setups. The most remarkable difference is present for low AoAs. A significant change in C_L slope is produced by the ZZ tape on the pressure side along with an increment of C_D. The pressure coefficient C_p distribution present in Figure 5, reveals a stalled flow on the airfoil pressure side. However, this stalled flow is not present at the ZZ tape location, it is at a streamwise location of 50%c. The ZZ tape beside forcing turbulent transition is inducing a pressure gradient which alters the recovering location of the flow downstream of it. By loss of energy, the flow separates at a location of 50%. This location fits with the beginning of the airfoil aft tail described by Timmer et al. [13].
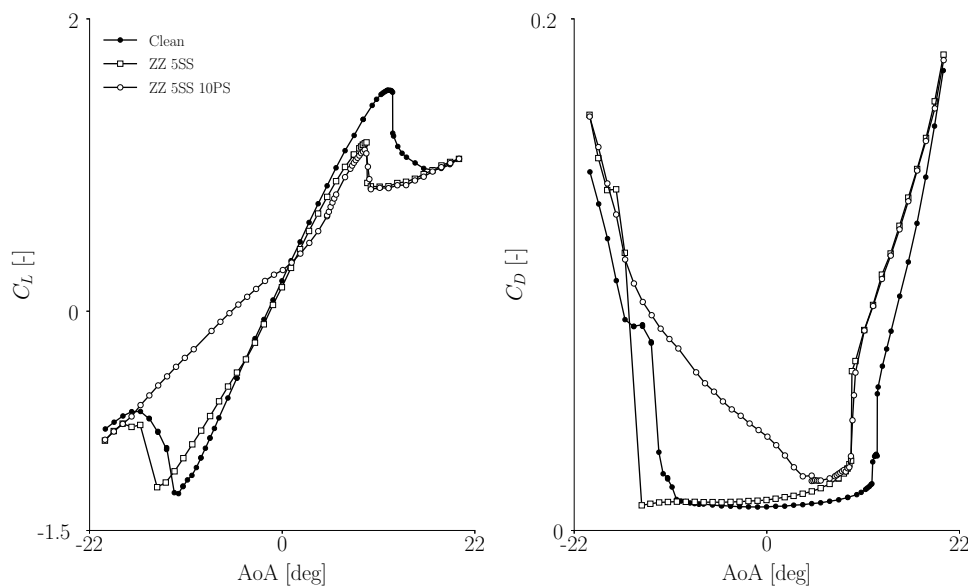

Figure 3. C_L and C_D polar curves for the different ZZ tape setups. In black the clean (smooth) surface state is taken as a reference.

3.2. Roughness method influence
The difference between using sandpaper to change the flow turbulence properties from the airfoil leading-edge and the ZZ tape for forcing turbulent boundary layer transition at its location is shown in Figure 4. A higher C_L drop and C_D increase are obtained in the sandpaper case for the positive AoA range. However, a similar performance between methods is obtained for low angles of attack. The stalled flow at pressure side in sandpaper test case is also related to the induced pressure gradient which is significant enough to separate the flow at the same position as in the ZZ tape test case.
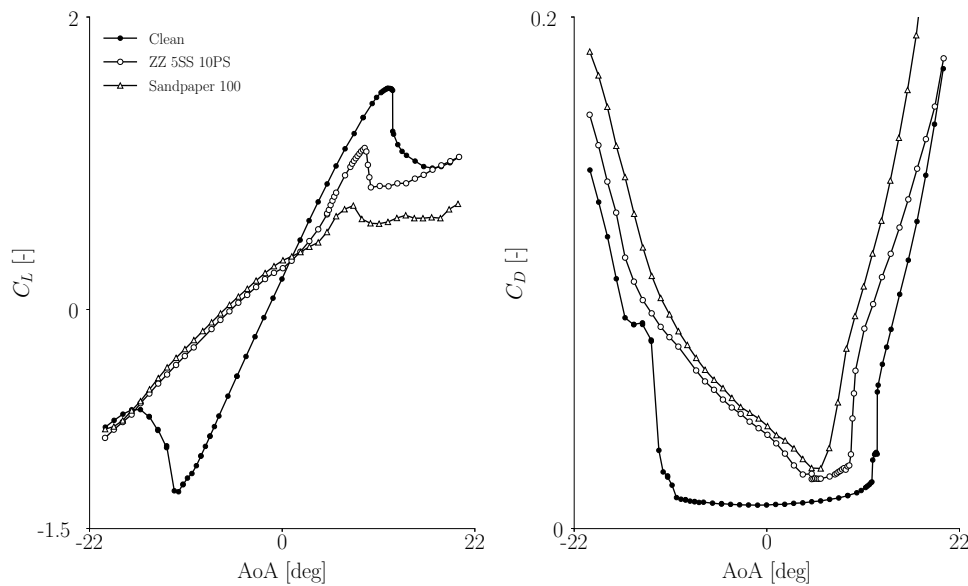
Figure 4. C_L and C_D polar curves comparison between 5SS 10PS ZZ tape setup and sandpaper method. In black the clean (smooth) surface state is taken as a reference.

The sandpaper C_L drop is more severe compared to the one obtained by O.Pires et al. [20] for an 18% thick airfoil. In fact, a dependant result on the pressure airfoil side was not obtained for the thinner airfoil because there was not present stalled flow on the airfoil pressure side.

The usage of sandpaper method provides comparable results to ZZ tapes until an angle of attack of 0°. For higher angles of attack significant differences are found in C_L and C_D. PIV measurements are a suitable option to obtain a more detailed view of the mean flow. In Figure 5 boundary layer profiles extracted from PIV measurements are shown. These profiles are represented in wall units using the estimated friction velocity (u_τ) value from the clean case. A least-squares methodology has been used to estimate the u_τ value. For each roughness method a displacement in U^+ is shown with respect to the clean test at the logarithmic region of the BL. This is in agreement with Schlichting experiments carried on a flat plate with distributed roughness elements [22]. However, Schlichting results showed a U^+ displacement conservative in curve shape. This condition is only fulfilled by the curve of the sandpaper test. A different physical modification of the BL is present depending on the method used.

3.3. Vortex generators performance
The previous assessment has revealed a significant dependence of the results on the roughness methods. A significant impact on the developed flow on the airfoil pressure side is also a key point for adapting the VGs use. Cases with perturbed flow on the pressure side are selected in order to optimize the VGs application locating VGs on both sides to suppress all possible stalled flow.

A streamwise position of 30%c was selected for VGs on the suction side according to D.Baldacchino [14] results. The position on the pressure side is based on the results presented in section 3.2. For ZigZag tape cases, a streamwise position of 40%c was considered suitable due to the previously observed C_p distribution. On the other hand, for sandpaper cases a higher C_L drop was present.

For all cases, VGs were able to increase the C_L value (see Figure 6) avoiding stall in the linear part of the clean curve. PIV measurements in Figure 7 correlates this expected effect as
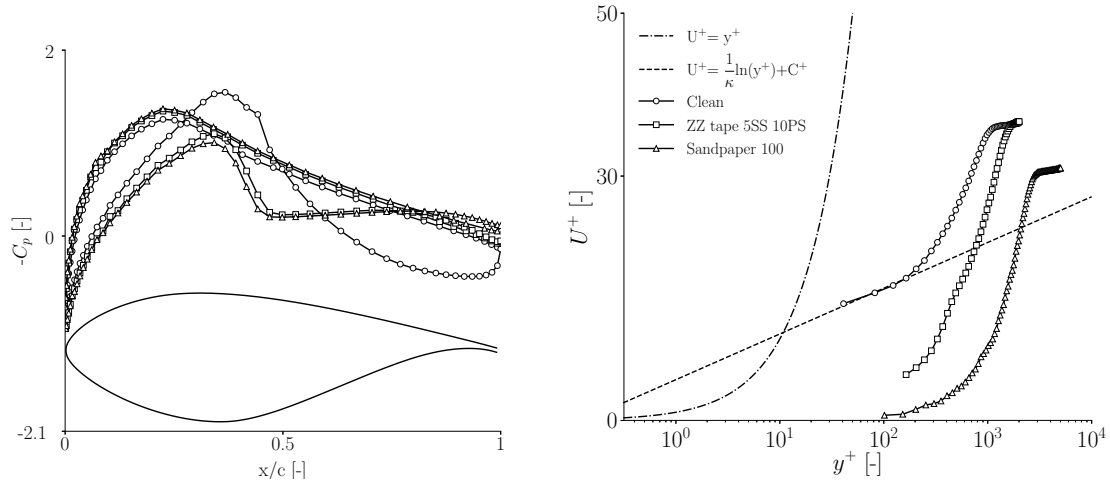
Figure 5. Left: C_p distribution comparative for AoA of 0º. Right: boundary layer in dimensional wall units extracted from PIV measurements at x/c = 0.85 for an AoA of 5º. A friction velocity value is estimated by least-square method using clean data (u_τ=1.56). The same value of u_τ is used for each line.
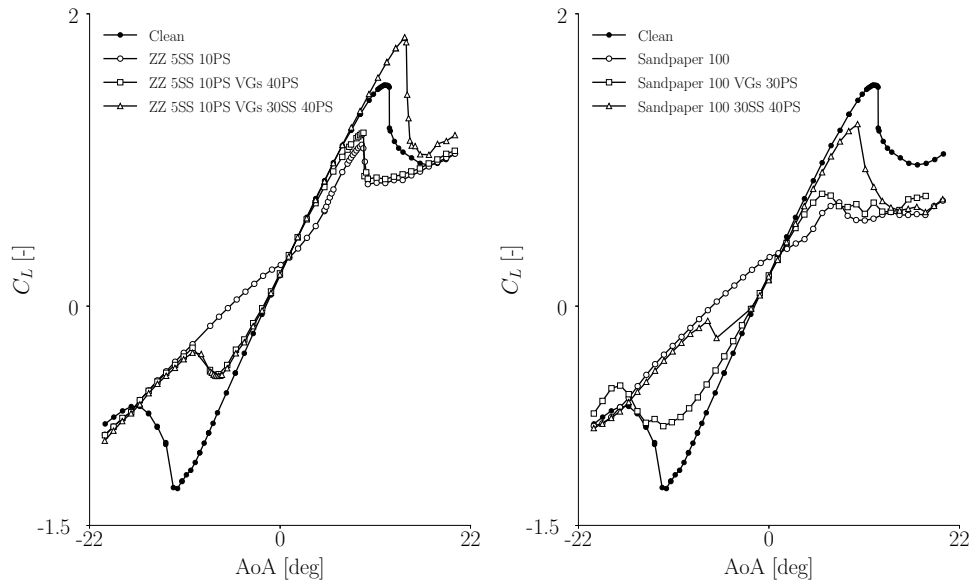

Figure 6. C_L polar curves for the different VGs setups under rough condition. ZZ tape cases on the left and sandpaper cases on the right.

a lower velocity deficit is observed in the case with VGs. In fact, the momentum exchange can be observed in the VGs wake until a streamwise location of 90%c.

It is important to remark that a recovery of C_L in positive angles of attack is obtained until 8º by the use of VGs on the airfoil pressure side (VGs 30PS and 40PS setups). Additionally, these VGs setups suppress the stalled flow in some part of the negative angle of attack region until negative trailing-edge stall is reached. This effect is more pronounced when VGs are located more upstream from 40PS to 30PS. These benefits can be combined with the stall delayed in the positive polar region once VGs are used on the suction side.

The associated drawback of using VGs is related to a C_D increment. This effect can be
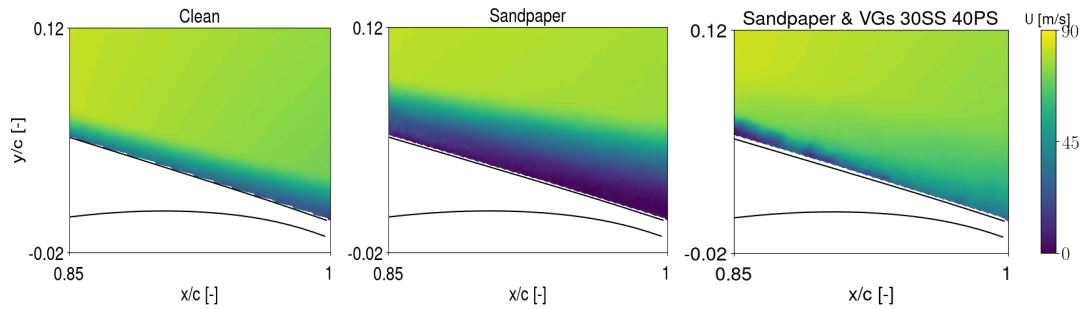
Figure 7. Stereostopic PIV velocity magnitude measurement for an angle of attack of 5º.

observed in Figure 8. A similar C_D increment is obtained compared to the one already introduced by the rough leading-edge. But, VGs on the pressure side ended up to be a suitable solution as for some angles of attack there is a lower C_D value compared to rough cases due to the stalled flow suppression on the pressure side. This improvement would not be possible if that need was not discovered and VGs would be used only on the suction side.
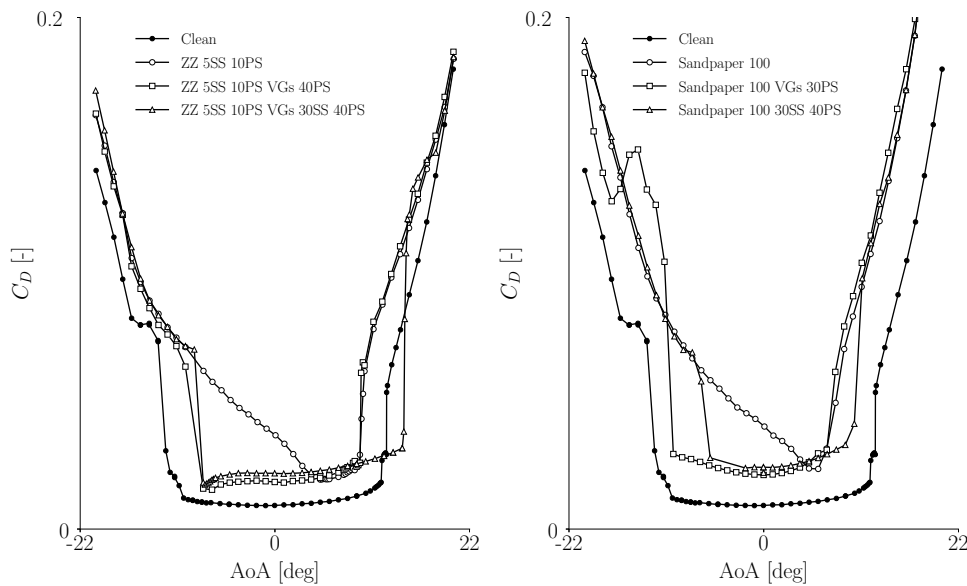

Figure 8. C_D polar curves for the different VGs setups under rough condition. ZZ tape cases on the left and sandpaper cases on the right.

4. Conclusions

The presented work is focused on evaluating the aerodynamic impact variation of a 30% thick airfoil produced by different roughness testing methods. For the most severe test cases, VGs have been used to improve the perturbed flow. Finally, the variability in airfoil aerodynamic performance is reduced once VGs are used.

As a result, some conclusions can be drawn:

- The configuration ZZ tapes 5SS 10PS is only representative concerning sandpaper once the stalled flow on the pressure side is present, but that is not the case for the rest of the polar curve. A higher deviation in the roughness impact is obtained for high AoAs.

- Boundary layer is physically modified in a different way depending on the roughness method. Only sandpaper produced a conservative shape U^+ displacement.

- VGs on the pressure side can also recover some lift loss for positive angles of attack.

- The increment in C_D produced by VGs is negligible compared to the already present by roughness. There is not a significant change in C_D due to the usage of VGs on the pressure side

A standard method for testing roughness should be found in order to ensure more precise comparisons between experiments. Uncertainties would be reduced and the use of add-ons would be also improved.

References

[1] Ehrmann R S. and White E B. and Maniaci D C. and Chow R and Langel C M. and Van Dam C P. 2013 *Realistic Leading-Edge Roughness Effects on Airfoil Performance* 31st Applied Aerodynamics Conf.

[2] Corten G P. and Veldkamp H F. 2001 Insects can halve wind-turbine power *Nature* **412** 41-42

[3] Zidane I. F. and Saqr K M. and Swadener G and Ma X and Shehadeh M F. 2016 On the role of surface roughness in the aerodynamic performance and energy conversion of horizontal wind turbine blades: a review. *Int. Journal of Energy Research* **40** 2054-2077

[4] Fuglsang P and Bak C and Gaunaa M and Antoniou I 2004 Design and Verification of the Risø-B1 Airfoil Family for Wind Turbines *Journal of Solar Energy Engineering* **126** 1002-1010

[5] Timmer W. A. and van Rooij R. P. J. O. M. 2019 *Summary of the Delft University Wind Turbine Dedicated Airfoils* Aerospace Sciences Meetings 41st Aerospace Sciences Meeting and Exhibit (Reno, Nevada)

[6] Wilcox B. and White E.B. and Maniaci D.C. 2017 *Roughness sensitivity Comparisons of Wind Turbine Blade Sections* Sandia National Laboratories (Albuquerque) NM. p. 118. SAND2017-11288

[7] Abbott I.H. and von Doenhoff A.E. 2012 *Theory of Wing Sections: Including a Summary of Airfoil Data* Dover Publications (New York)

[8] Mendez B and Muñoz A and Pires O and Munduate X 2017 *Characterization of the carborundum used in rough airfoil surface tests and modelling with CFD* 35th Wind Energy Symp. (Grapevine, Texas) 0916

[9] van Rij J. A. and Belnap B. J. and Ligrani P. M. 2002 Analysis and Experiments on Three-Dimensional, Irregular Surface Roughness *Journal of Fluids Engineering* **124** 671-677

[10] Turner A.B. and Hubbe-Walker S.E. and Bayley F.J. 2000 Fluid flow and heat transfer over straight and curved rough surfaces *Int. Journal of Heat and Mass Transfer* **43** 251-262

[11] Kerho M and Bragg M 2012 *Effect of large distributed leading-edge roughness on boundary layer development and transition* 13th Applied Aerodynamics Conf. (San Diego,CA,U.S.A.)

[12] Bragg M.B. and Broeren A.P. and Blumenthal L.A. 2005 Iced-airfoil aerodynamics *Progress in Aerospace Sciences* **41** 323 - 362

[13] van Rooij R. P. J. O. M. and Timmer W. A. 2003 Roughness Sensitivity Considerations for Thick Rotor Blade Airfoils *Journal of Solar Energy Engineering* **125** 468

[14] Baldacchino D and Ferreira C and De Tavernier D and Timmer W.A. and van Bussel G. J. W. 2018 Experimental parameter study for passive vortex generators on a 30% thick airfoil *Wind Energy* **21** 745-765

[15] Skrzypiński W and Gaunaa M and Back C 2014 The Effect of Mounting Vortex Generators on the DTU 10MW Reference Wind Turbine Blade *Journal of Physics: Conf. Series* **524** 12034

[16] Anderson J.D. 2010 *Fundamentals of Aerodynamics* McGraw-Hill Education (New York)

[17] Ragni D and Ferreira C 2016 Effect of 3D stall-cells on the pressure distribution of a laminar NACA64-418 wing *Experiments in Fluids* **57** 127

[18] Ragni D. and Schrijer F. and van Oudheusden B. W. and Scarano F. 2011 Particle tracer response across shocks measured by PIV *Experiments in Fluids* **50** 53-64

[19] Braslow A. L. and Knox E. C. 1958 Simplified Method for Determination of Critical Height of Distributed Roughness Particles for Boundary-layer Transition at Mach Numbers from 0 to 5 National Advisory Committee for Aeronautics. Langley Aeronautical Lab. (Langley Field, VA, United States)

[20] Pires O and Munduate X and Boorsma K and Ceyhan O and Madsen H A. and Timmer W.A. 2018 Experimental investigation of Surface Roughness effects and Transition on Wind Turbine performance *Journal of Physics: Conf. Series* **1037** 052018

[21] FEPA 2006 *FEPA-Standard 42-1:2006: Grains of fused aluminium oxide, silicon carbide and other abrasive materials for coatedabrasives Macrogrits P 12 to P 220*

[22] Mayes C. and Schlichting H. and Krause E. and Oertel H.J. and Gersten K. 2003 *Boundary-Layer Theory* Springer (Berlin, Heidelberg)